2015

# Robust Optimization for Bidirectional Dispatch Coordination of Large-Scale V2G

Xiaoqing Bai
*University of Nebraska-Lincoln*, xbai2@unl.edu

Wei Qiao
*University of Nebraska-Lincoln*, wqiao@engr.unl.edu

Year: 2015, Volume: PP, Issue: 99
Pages: 1 - 1, DOI: 10.1109/TSG.2015.2396065

# Robust Optimization for Bidirectional Dispatch Coordination of Large-Scale V2G

Xiaoqing Bai and Wei Qiao, *Senior Member, IEEE*

***Abstract*—This paper proposes a robust optimization (RO) model for bidirectional dispatch coordination of large-scale plug-in electric vehicles (PEVs) in a power grid in which the PEVs are aggregated to manage. The PEV aggregators are considered as a type of dispatchable demand response and energy storage resource with stochastic behaviors, and can supply load or provide ancillary services such as regulation reserve to the grid. The proposed RO model is then reformulated as a mixed-integer quadratic programming model, which can be solved efficiently. Computer simulations are performed for a power grid with ten generators and three PEV aggregators to validate the economic benefit of the RO model for bidirectional dispatch coordination of the PEVs and the robustness of the RO model to the uncertainty of the PEVs' stochastic mobility behaviors.**

***Index Terms*—Bidirectional dispatch, coordination, plug-in electric vehicle (PEV), robust optimization (RO), smart grid, vehicle to grid (V2G).**

## NOMENCLATURE

*Indices*

- $i$ Index of thermal generators.
- $j$ Index of plug-in electric vehicle (PEV) aggregators.
- $t$ Index of time intervals during a dispatch period.
- $T$ Total number of intervals for a dispatch period.
- $n$ Number of thermal generators.
- $m$ Number of PEV aggregators.

*Parameters*

- $a_{1i}, a_{2i}, a_{3i}$ Fuel cost coefficients of thermal generator $i$.
- $\sigma t$ Number of hours during each dispatch interval $t$.
- $p_{ec,t}$ Capability unit price of reserve during $t$.
- $\mathrm{LMP}_{j,t}$ Locational marginal price (LMP) of PEV aggregator $j$ during $t$.
- $k_i^{\mathrm{up}}/k_i^{\mathrm{down}}$ Start-up/down cost of thermal generator $i$.
- $P_t^{\mathrm{load}}$ Base load without PEV aggregators during $t$.
- $\underline{P_i}/\overline{P_i}$ Lower/upper active power limit of generator $i$.
- $\underline{R_i^{\mathrm{down}}}/R_i^{\mathrm{up}}$ Ramp-down/up limit of generator $i$.
- $H_i^{\mathrm{down}}/H_i^{\mathrm{up}}$ Minimum down/up time limit of generator $i$.
- $\mathrm{POR}_{i,t}$ Preference of generator $i$ to provide reserve during $t$ (1 if it prefers; otherwise 0).
- $\overline{P}_j^{\mathrm{chg}}/\overline{P}_j^{\mathrm{dis}}$ Limits of charging/discharging power of PEV aggregator $j$, which are determined by the maximum charging/discharging power of the PEVs in the aggregator as well as the physical interface (e.g., chargers and power line capacities) between PEV aggregator $j$ and the power grid.
- $\mathrm{PIO}_{j,t}$ Status of PEV aggregator $j$ to participate in grid operation to charge, discharge to supply load, or provide regulation reserve during $t$.
- $\eta_j^{\mathrm{chg}}/\eta_j^{\mathrm{dis}}$ Charging/discharging efficiency of PEV aggregator $j$.
- $\overline{w}_{j,t}^{\mathrm{SoC}}$ Maximum energy capacity of PEV aggregator $j$ during $t$.
- $w_{j,t}^{\mathrm{SoC}}$ Predicted available energy capacity of PEV aggregator $j$ during $t$.
- $E_j^{\mathrm{Con}}$ The total energy consumed by aggregator $j$ for driving in $T$.
- $\overline{E}_j^{\mathrm{SoC}}$ Maximum energy capacity of PEV aggregator $j$.
- $R^{\mathrm{min}}$ General minimum active power requirement of a regulation provider specified by the grid operator.
- SR Reserve requirement.
- $\tau$ Maximum time allowed for a thermal generator to ramp up to deliver the committed reserve capacity.

*Cost Variables*

- $\mathrm{CF}_t$ Total fuel cost of all thermal generators during $t$.
- $\mathrm{CR}_t$ Total cost of thermal generators to provide reserve service during $t$.
- $\mathrm{CO}_t$ Total cost of starting up and shutting down thermal generators during $t$.
- $\mathrm{PR}_t$ Total cost for PEV aggregators to provide the regulation reserve service during $t$.
- $\mathrm{PS}_t$ Total cost for PEV aggregators to discharge power to the power grid during $t$.

*Decision Variables*

- $P_{i,t}$ Active power of thermal generator $i$ during $t$.
- $u_{i,t}$ Unit commitment (UC) status (0/1) of thermal generator $i$ during $t$.
- $o_{i,t}/v_{i,t}$ Unit start-up/shut-down status (0/1) of thermal generator $i$ during $t$.

Manuscript received May 11, 2014; revised October 20, 2014 and January 8, 2015; accepted January 20, 2015. This work was supported in part by the U.S. National Science Foundation under CAREER Award ECCS-0954938, and in part by the National Natural Science Foundation of China under Grant 51367004. Paper no. TSG-00401-2014.

The authors are with the Power and Energy Systems Laboratory, Department of Electrical and Computer Engineering, University of Nebraska–Lincoln, Lincoln, NE 68588-0511 USA (e-mail: xbai2@unl.edu; wqiao@engr.unl.edu).

Color versions of one or more of the figures in this paper are available online at http://ieeexplore.ieee.org.

Digital Object Identifier 10.1109/TSG.2015.2396065

$P_{j,t}^{\text{chg}}/P_{j,t}^{\text{dis}}$ Charging/discharging power of PEV aggregator $j$ during $t$.

$z_{j,t}^{\text{chg}}/z_{j,t}^{\text{dis}}$ Charging/discharging status (0/1) of PEV aggregator $j$ during $t$.

$R_{j,t}^{c}/R_{j,t}^{d}$ Reserve capacity of PEV aggregator $j$ in the charging/discharging mode during $t$.

$z_{j,t}^{c\text{Res}}/z_{j,t}^{d\text{Res}}$ Status (0/1) of PEV aggregator $j$ in the charging/discharging mode to provide regulation reserve service during $t$.

*Uncertainty-Related Variables*

$\tilde{w}_{j,t}^{\text{SoC}}$ Uncertain available energy capacity of PEV aggregator $j$ during $t$.

$\gamma_{j,t}$ Degree of uncertainty of the available energy capacity of PEV aggregator $j$ during $t$ and $|\gamma_{j,t}| \leq 1$.

$\mathcal{R}_{j}^{\text{SoC}}$ Uncertainty set of $\tilde{w}_{j}^{\text{SoC}}$ for aggregator $j$.

*Uncertainty-Related Parameters*

$\alpha$ Degree of variation of $\tilde{w}_{j,t}^{\text{SoC}}$ from $\underline{w}_{j,t}^{\text{SoC}}$.

$\Gamma_j$ Budget of uncertainty of the PEV aggregator $j$, which is the maximum level of uncertainty of the available energy capacity that the PEV aggregator $j$ is willing to tolerate, where $1/T\|\gamma_{j,t}\|_1 \leq \Gamma_j$, $t = 1, \ldots, T$, $0 \leq \Gamma_j \leq 1$.

## I. Introduction

ECONOMIC and environmental incentives and advances in technology are driving dramatic changes in modern electric power grid. One of the changes are PEVs, which will offer customers a promising way to save gasoline cost, and help reduce carbon emissions as well as other pollutants. In addition to economic and environmental benefits, PEVs also offer a potential source of energy storage, which is valuable to the electric power grid. The possibility of using PEV batteries to provide ancillary services to support electric grids has been studied for more than one decade [1].

Although PEVs are still in the development stage, much work has been conducted to analyze the impact of PEVs on the electric power grids from the energy, environmental, and economic points of view [2]–[4]. Through the vehicle to grid (V2G) technology, the parked PEVs within a certain area can constitute a PEV aggregator when they are connected to the grid through some intelligent equipment. Such a PEV aggregator can represent a well-defined responsive load and offer additional generation capacity for the provision of ancillary services for the power grids [5], [6]. Some research has been conducted on mathematical models and control algorithms for operation of V2G and the associated power grids. For example, in [7], an optimal V2G aggregator was designed for frequency regulation, where the dynamic programming method was used to obtain the optimal charging control for each PEV. In [8], an optimal charging strategy for PEVs in a market environment was obtained by using a quadratic programming method. In [9], the particle swarm optimization technique was used to minimize the fuel cost and emission in a power grid, where the V2G was operated either as load or energy storage.

However, [1]–[4] focused on creating mathematical models and control algorithms based on the traditional deterministic optimization (DO)-based power dispatch frameworks without considering the operating characters of the PEV aggregators [3], such as fast response, short duration, stochastic mobility of the PEVs within an aggregator, etc. Moreover, in most of the prior work, to make the models easy to solve, the active powers of the PEV aggregators were considered as continuous variables and the energy losses were ignored during the charging and discharging operations. In practice, the charging and discharging operations of a PEV aggregator cannot happen at the same time from the electric power grid's point of view. Furthermore, energy losses are always involved in the charging and discharging processes of PEVs and the charging and discharging efficiencies may be different. To overcome these limitations, in this paper, the charging and discharging powers of a PEV aggregator are represented by different variables using mixed-integer constraints to better handle the aforementioned practical issues.

Based on the current technology, if a PEV has available charging/discharging capacity, it can be charged/discharged when it is parked and connected to the grid through some charging/discharging equipment. Obviously, the available charging/discharging capacity of a PEV aggregator depends on the maximum energy capacity and the available energy capacity (i.e., the total usable energy stored in the PEV batteries) of the PEV aggregator as well as the stochastic mobility behaviors of the PEVs in the aggregator. Stochastic optimization approaches have been used to model the V2G dispatch problem in ancillary markets [6], [10], in which the stochastic behaviors of PEVs were modeled by using probability distributions. Unfortunately, it is usually difficult to identify accurate probability distributions for the uncertainties of the available charging/discharging capacities of a PEV aggregator due to the lack of historical data. A scenario-based stochastic model was presented in [11] to solve the problem of operation coordination of PEVs and wind power generation. To obtain an accurate solution, a large number of scenarios are required, which needs intensive computational cost.

In contrast to the stochastic optimization approaches, the robust optimization (RO) approach [12] does not model the probability distribution, but only requires moderate information of the uncertainty, such as the mean and the upper and lower limits of the uncertainty. Furthermore, the optimal solution generated from a RO model covers all realizations of the uncertainty over a specific set designed. Recently, the RO approach has been applied to solve the problems of generation expansion planning [13] and UC [14]–[16], in which the uncertainties of load demand and/or new energy resources were considered.

This paper extends the classical UC model to propose a DO model for bidirectional dispatch (i.e., charging and discharging) coordination of large-scale V2G in a power grid. Based on the DO model, an RO model is then proposed by constructing the available energy capacities of the PEV aggregators for each dispatch interval as an uncertainty set according to the stochastic mobility behaviors of the PEVs. The proposed RO model is then reformulated as a deterministic mixed-integer quadratic programming problem, which can be solved efficiently by using an existing solver, such as CPLEX [17] or Gurobi [18]. Simulation studies are conducted for a power

grid with ten thermal generators and three PEV aggregators to validate the economic benefit and robustness of the proposed RO model.

## II. Proposed RO Model for Bidirectional Dispatch Coordination of V2G

### A. Problem Description

Consider a power grid with large-scale V2G. An entity who operates PEV charging/discharging facilities and participates in the grid operation, such as a distribution system operator, collects the operation preference of each PEV in a certain area within its territory to generate an aggregated operation preference for all the PEVs, i.e., a PEV aggregator, in that area. The size of the aggregator fleet depends on the population, the number of PEVs, and the number of charging/discharging facilities in the area. The information of the PEV aggregator is shared with the grid operator, such as an independent system operator. The grid operator includes the PEV aggregators into its resource commitment and economic dispatch routine, where each PEV aggregator is considered as a type of demand response and energy storage resource, but its primary function is for transportation. This section proposes a RO-based UC model for day-ahead (DA) operation planning of large-scale V2G in a power grid. First, a DO-based UC model is designed for dispatch coordination of the PEV aggregators. Next, the uncertainty sets of the problem are constructed. Based on the DO model and the uncertainty sets, the RO model is formulated and is then converted to a deterministic mixed-integer quadratic programming problem, which can be solved efficiently.

### B. DO Model Formulation

When a PEV aggregator participates in the grid operation, it can absorb energy from or feed energy back to the grid for shifting the peak load or eliminating the violation of generator ramps. Furthermore, the available energy capacity of a PEV aggregator can be used to provide spinning/regulation reserve service if necessary. Therefore, when participating in the grid operation, a PEV aggregator has four operating modes: charging, discharging to supply load, providing regulation reserve in the charging status, and providing regulation reserve in the discharging status. The four operating modes are represented by four binary (0/1) variables and the logical relations among them are formulated as the mixed-integer constraints in the model. In this paper, the predicted regulation market capability prices and LMPs are used as the reserve capability unit prices and discharging energy unit prices of the PEV aggregators, respectively.

The objective of the proposed model is to minimize the total cost of all thermal generators and all PEV aggregators in a given dispatch period $T$. The total cost of all thermal generators includes the costs of fuel ($\mathrm{CF}_t$), reserve capacity provided ($\mathrm{CR}_t$), and operation ($\mathrm{CO}_t$) during $T$. The total cost of all PEV aggregators includes the costs for the reserve capacity provided ($\mathrm{PR}_t$) and discharging power ($\mathrm{PS}_t$) during $T$. The proposed DO model is formulated by integrating the PEV aggregators into a classical UC model in [19] as follows, where the objective function is

$$\min \sum_{t=1}^{T} \mathrm{CF}_t + \mathrm{CR}_t + \mathrm{CO}_t + \mathrm{PR}_t + \mathrm{PS}_t \tag{1}$$

where

$$\mathrm{CF}_t = \sum_{i=1}^{n} a_{1i} P_{i,t}^2 + a_{2i} P_{i,t} + a_{3i}$$

$$\mathrm{CR}_t = p_{ec,t} \sum_{i=1}^{n} \mathrm{POR}_{i,t} \left( \min \left( u_{i,t} \left( \overline{P_i} - P_{i,t} \right), u_{i,t} \tau R_i^{\mathrm{up}} \right) \right)$$

$$\mathrm{CO}_t = \sum_{i=1}^{n} k_i^{\mathrm{up}} o_{i,t} + \sum_{i=1}^{n} k_i^{\mathrm{down}} v_{i,t}$$

$$\mathrm{PR}_t = p_{ec,t} \sum_{j=1}^{m} \mathrm{PIO}_{j,t} \left( z_{j,t}^{d\mathrm{Res}} R_{j,t}^{d} + z_{j,t}^{c\mathrm{Res}} R_{j,t}^{c} \right)$$

$$\mathrm{PS}_t = \sum_{j=1}^{m} \mathrm{PIO}_{j,t} \mathrm{LMP}_{j,t} P_{j,t}^{\mathrm{dis}}$$

where $\mathrm{PIO}_{j,t} = 1$ if the PEV aggregator $j$ participates in the grid operation during $t$; $\mathrm{PIO}_{j,t} = 0$ if the PEV aggregator $j$ is included in the base load instead of being dispatched during $t$.

The optimization is subject to the following constraints, where $i = 1, \ldots, n$; $j = 1, \ldots, m$; *and* $t = 1, \ldots, T$.

1) Active power balance during $t$

$$\sum_{i=1}^{n} u_{i,t} P_{i,t} + \sum_{j=1}^{m} \left( P_{j,t}^{\mathrm{dis}} - P_{j,t}^{\mathrm{chg}} \right) - P_t^{\mathrm{load}} = 0. \tag{2}$$

2) Operating and ramping limits of each generator

$$u_{i,t} \underline{P_i} \le P_{i,t} \le u_{i,t} \overline{P_i} \tag{3}$$

$$R_i^{\mathrm{down}} \le P_{i,t} - P_{i,t-1} \le R_i^{\mathrm{up}}. \tag{4}$$

3) Minimum up and down time limits of generators [20]

$$-u_{i,t-1} + u_{i,t} - u_{i,k} \le 0, \ k = t, \ldots, \ H_i^{\mathrm{up}} + t - 1 \tag{5}$$

$$u_{i,t-1} - u_{i,t} + u_{i,k} \le 1, \ k = t, \ldots, \ H_i^{\mathrm{down}} + t - 1 \tag{6}$$

$$-u_{i,t-1} + u_{i,t} - o_{i,t} \le 0 \tag{7}$$

$$u_{i,t-1} - u_{i,t} - v_{i,t} \le 0. \tag{8}$$

4) Reserve requirement

$$\mathrm{SR} \le \sum_{i=1}^{n} \mathrm{POR}_{i,t} \left( \min \left( u_{i,t} \left( \overline{P_i} - P_{i,t} \right), u_{i,t} \tau R_i^{\mathrm{up}} \right) \right) + \sum_{i=1}^{m} \mathrm{PIO}_{j,t} \left( z_{j,t}^{d\mathrm{Res}} R_{j,t}^{d} + z_{j,t}^{c\mathrm{Res}} R_{j,t}^{c} \right). \tag{9}$$

5) Logical relations of the status of charging, discharging, and providing reserve of each PEV aggregator

$$z_{j,t}^{\mathrm{chg}} + z_{j,t}^{\mathrm{dis}} \le 1 \tag{10}$$

$$z_{j,t}^{\mathrm{chg}} + z_{j,t}^{d\mathrm{Res}} \le 1 \tag{11}$$

$$z_{j,t}^{\mathrm{dis}} + z_{j,t}^{c\mathrm{Res}} \le 1 \tag{12}$$

$$z_{j,t}^{d\mathrm{Res}} + z_{j,t}^{c\mathrm{Res}} \le 1. \tag{13}$$

6) Charging and discharging power limits of each aggregator

$$0 \le P_{j,t}^{\text{chg}} \le \text{PIO}_{j,t} z_{j,\text{t}}^{\text{chg}} \overline{P}_{j,t}^{\text{chg}} \tag{14}$$

$$0 \le P_{j,t}^{\text{dis}} \le \text{PIO}_{j,t} z_{j,t}^{\text{dis}} \overline{P}_{j,t}^{\text{dis}}. \tag{15}$$

7) Charging and discharging energy limits of each aggregator

$$0 \le P_{j,t}^{\text{chg}} \sigma t \le \text{PIO}_{j,t} z_{j,t}^{\text{chg}} \left( \overline{w}_{j,t}^{\text{SoC}} - w_{j,t}^{\text{SoC}} \right) \tag{16}$$

$$0 \le P_{j,t}^{\text{dis}} \sigma t \le \text{PIO}_{j,t} z_{j,t}^{\text{dis}} w_{j,t}^{\text{SoC}} \tag{17}$$

where the term ($\overline{w}_{j,t}^{\text{SoC}}$- $w_{j,t}^{\text{SoC}}$) represents the available charging capacity of the PEV aggregator $j$ during $t$.

8) Reserve capacity limits of aggregator $j$ in the discharging mode during $t$

$$0 \le R_{j,t}^{d} \le \text{PIO}_{j,t} \min\left( \overline{P}_{j,t}^{\text{dis}} - P_{j,t}^{\text{dis}}, \frac{w_{j,t}^{\text{SoC}}}{\sigma t} - P_{j,t}^{\text{dis}} \right) \tag{18}$$

where $w_{j,t}^{\text{SoC}}/\sigma t$ represents the maximum discharging power limited by the available energy capacity of the PEV aggregator $j$ during $t$; $\min(\overline{P}_{j,t}^{\text{dis}} - P_{j,t}^{\text{dis}}, (w_{j,t}^{\text{SoC}}/\sigma t) - P_{j,t}^{\text{dis}})$ represents the available reserve capacity provided by the PEV aggregator $j$ during $t$ when it is in the discharging status.

9) Reserve capacity limits of aggregator $j$ in the charging mode during $t$

$$0 \le R_{j,t}^{c} \le \text{PIO}_{j,t} P_{j,\text{t}}^{\text{chg}}. \tag{19}$$

10) Minimum requirement of regulation reserve of each PEV aggregator in the discharging status

$$z_{j,\text{t}}^{d\text{Res}} = 0 \text{ if } \min\left( \overline{P}_{j,t}^{\text{dis}} - P_{j,t}^{\text{dis}}, \frac{w_{j,t}^{\text{SoC}}}{\sigma t} - P_{j,t}^{\text{dis}} \right) < R^{\min}. \tag{20}$$

11) Minimum requirement of regulation reserve of each PEV aggregator in the charging status

$$z_{j,t}^{c\text{Res}} = 0 \text{ if } P_{j,t}^{\text{chg}} < R^{\min} \tag{21}$$

$$z_{j,t}^{c\text{Res}} = 0 \text{ if } P_{j,t}^{\text{chg}} + \frac{w_{j,t}^{\text{SoC}}}{\sigma t} > \overline{w}_{j,t}^{\text{SoC}}. \tag{22}$$

12) Energy balance of each PEV aggregator over $T$

$$\sum_{t=1}^{T} \eta_j^{\text{chg}} P_{j,t}^{\text{chg}} \sigma t = E_j^{\text{Con}} + \sum_{t=1}^{T} \eta_j^{\text{dis}} P_{j,t}^{\text{dis}} \sigma t. \tag{23}$$

The solution to the proposed model (1)–(23) provides the grid operator with the optimal operation schedules for the thermal generators and PEV aggregators over the dispatch period. However, some parameters of this model are uncertain, such as the available energy capacity of each PEV aggregator due to the stochastic behaviors of PEVs. Therefore, the solution to the DO model (1)–(23) will not be optimal. In this paper, an RO model is proposed to handle the parameter uncertainties.

### C. Uncertainty Set

The uncertain parameters in the DO model (1)–(23) include the available energy capacity of each PEV aggregator ($w_{j,t}^{\text{SoC}}$), reserve capability unit prices ($p_{ec,t}$), LMPs ($\text{LMP}_{j,t}$), and system base load ($P_t^{\text{load}}$) during each $t$. The values of $p_{ec,t}$, $\text{LMP}_{j,t}$, and $P_t^{\text{load}}$ can be forecasted with acceptable accuracy by using a time series prediction method, such as the autoregressive integrated moving average (ARIMA) method [21], owing to the availability of abundant historical data. However, it is unsuitable to use any time series prediction method to predict $w_{j,t}^{\text{SoC}}$ and its level of uncertainty is much higher than those of $p_{ec,t}$, $\text{LMP}_{j,t}$, and $P_t^{\text{load}}$ in this paper because no historical data of $w_{j,t}^{\text{SoC}}$ are currently available. Therefore, for the sake of simplicity, in this paper, only the available energy capacity of each PEV aggregator during $t$ is considered an uncertain parameter, which is denoted as $\tilde{w}_{j,t}^{\text{SoC}}$. However, the uncertainties of $p_{ec,t}$, $\text{LMP}_{j,t}$, and $P_t^{\text{load}}$ can be considered in the same way.

The uncertainty set [12] $\mathcal{R}_j^{\text{SoC}}$ of $\tilde{w}_{j,t}^{\text{SoC}}$ for the aggregator $j$ in a given dispatch period $T$ is defined as follows:

$$\begin{aligned} &\mathcal{R}_j^{\text{SoC}}\left(\alpha, \Gamma_j, w_{j,t}^{\text{SoC}}\right) \\ &:= \Bigg\{ \tilde{w}_{j,t}^{\text{SoC}} : \exists \gamma_{j,t} \in \mathbb{R}^T \text{ s.t. } \tilde{w}_{j,t}^{\text{SoC}} \in \Big[ w_{j,t}^{\text{SoC}} - \alpha w_{j,t}^{\text{SoC}} \left|\gamma_{j,t}\right|, \\ &\qquad\qquad w_{j,t}^{\text{SoC}} + \alpha w_{j,t}^{\text{SoC}} \left|\gamma_{j,t}\right| \Big], \\ &\qquad \left|\gamma_{j,t}\right| \le 1, \ \frac{1}{T} \sum_{t=1}^{T} \left|\gamma_{j,t}\right| \le \Gamma_j \Bigg\}. \end{aligned} \tag{24}$$

The set $\mathcal{R}_j^{\text{SoC}}$ considers all possible available energy capacity values of the PEV aggregator $j$ in the range $[w_{j,t}^{\text{SoC}} - \alpha w_{j,t}^{\text{SoC}} |\gamma_{j,t}|, w_{j,t}^{\text{SoC}} + \alpha w_{j,t}^{\text{SoC}} |\gamma_{j,t}|]$ with the constraint that the average degree of uncertainties of $w_{j,t}^{\text{SoC}}$ over the dispatch period $T$ is no more than $\Gamma_j$. Thus, the value of $\alpha \cdot \Gamma_j$ represents the uncertainty level of $\mathcal{R}_j^{\text{SoC}}$, where a larger value of $\alpha \cdot \Gamma_j$ indicates a higher level of uncertainty.

Since $|\gamma_{j,t}| \le 1$ and $1/T \|\gamma_{j,t}\|_1 \le \Gamma_j$, when $\Gamma_j = 0$, the set (24) is a singleton $\{w_{j,t}^{\text{SoC}}, j = 1, \ldots m; t = 1, \ldots, T\}$, which corresponds to the nominal deterministic case. As $\Gamma_j$ increases, the range of the uncertainty set $\mathcal{R}_j^{\text{SoC}}$ enlarges. It means that a larger deviation of the total available energy capacity from the predicted value is considered for the PEV aggregator $j$. Then, the resulting RO model is more conservative, and the system is protected against a higher degree of uncertainty. When $\Gamma_j = 1$, $\mathcal{R}_j^{\text{SoC}}$ only depends on $w_{j,t}^{\text{SoC}}$ and $\alpha$.

### D. RO Model Formulation

Define $\boldsymbol{x} = [P_{i,t}, u_{i,t}, o_{i,t}, v_{i,t}, P_{j,t}^{\text{chg}}, z_{j,t}^{\text{chg}}, P_{j,t}^{\text{dis}}, z_{j,t}^{\text{dis}}, z_{j,t}^{d\text{Res}}, z_{j,t}^{c\text{Res}}] (i = 1, \ldots, n; \ j = 1, \ldots, m; \ t = 1, \ldots, T)$ the vector of decision variables, where $P_{i,t}$, $P_{j,t}^{\text{chg}}$, and $P_{j,t}^{\text{dis}}$ are continuous variables, and the others are binary (0/1) variables. The DO model (1)–(23) can be expressed in the following form:

$$\begin{aligned} &\min_{\boldsymbol{x}} \ f(\boldsymbol{x}) \\ &\text{s.t } g(\boldsymbol{x}) \preccurlyeq 0 \end{aligned} \tag{25}$$

where $\preccurlyeq$ means that there are both inequality and equality constraints.

Then, define $\boldsymbol{w} = [\gamma_{j,t}](j = 1, \ldots, m;\ t = 1, \ldots, T)$, the set of uncertainty parameters and $\mathcal{R}^{\mathrm{SoC}} = \prod_{j=1}^{m} \mathcal{R}_j^{\mathrm{SoC}}$, the following RO model [12] can be formulated based on (25):

$$\begin{aligned} &\min_{\boldsymbol{x}} \ \max_{\boldsymbol{w}} \ f(\boldsymbol{x}, \boldsymbol{w}) \\ &\text{s.t. } g(\boldsymbol{x}, \boldsymbol{w}) \preccurlyeq 0 \ \forall \boldsymbol{w} \in \mathcal{R}^{\mathrm{SoC}} \end{aligned} \tag{26}$$

where $w_{j,t}^{\mathrm{SoC}}$ in (16)–(18), (20), and (22) is replaced with $\tilde{w}_{j,t}^{\mathrm{SoC}}$.

The RO model (26) takes into account all possible scenarios of $\tilde{w}_{j,t}^{\mathrm{SoC}}$ using the uncertainty set $\mathcal{R}_j^{\mathrm{SoC}}$. The solution of (26) is therefore feasible and robust for any realization of the uncertain available energy capacities of the PEV aggregators. In contrast, the solution of the DO model (25) only guarantees the feasibility for a single nominal realization of $\tilde{w}_{j,\mathrm{t}}^{\mathrm{SoC}}$; while the stochastic optimization method only considers a finite number of scenarios of $\tilde{w}_{j,t}^{\mathrm{SoC}}$.

## III. Solution Method to the RO Model

The robust counterpart approach [22] is applied to solve the proposed RO model. The paradigm is to convert the RO model (26) to a computable model called the robust counterpart by removing the uncertainties using the method such as explicit maximization, duality properties, or relaxation. The explicit maximization method is used to remove the uncertainties in this paper because (24) belongs to a typical norm-ball constraint.

The constraints of the problem (26) involving uncertainties are the charging/discharging energy and regulation requirement limits of each PEV aggregator below. They are not computable

$$0 \le P_{j,t}^{\mathrm{chg}} \sigma t \le \mathrm{PIO}_{j,t} z_{j,t}^{\mathrm{chg}} \left( \overline{w}_{j,t}^{\mathrm{SoC}} - \tilde{w}_{j,t}^{\mathrm{SoC}} \right) \tag{27}$$

$$0 \le P_{j,t}^{\mathrm{dis}} \sigma t \le \mathrm{PIO}_{j,t} z_{j,t}^{\mathrm{dis}} \tilde{w}_{j,t}^{\mathrm{SoC}} \tag{28}$$

$$0 \le R_{j,t}^{d} \le \mathrm{PIO}_{j,t} \min \left( \overline{P}_{j,t}^{\mathrm{dis}} - P_{j,t}^{\mathrm{dis}}, \frac{\tilde{w}_{j,t}^{\mathrm{SoC}}}{\sigma t} - P_{j,t}^{\mathrm{dis}} \right) \tag{29}$$

$$z_{j,t}^{d\mathrm{Res}} = 0 \text{ if } \min \left( \overline{P}_{j,t}^{\mathrm{dis}} - P_{j,t}^{\mathrm{dis}}, \tilde{w}_{j,t}^{\mathrm{SoC}} / \sigma t - P_{j,t}^{\mathrm{dis}} \right) < R^{\min} \tag{30}$$

$$z_{j,t}^{c\mathrm{Res}} = 0 \text{ if } P_{j,t}^{\mathrm{chg}} + \frac{\tilde{w}_{j,t}^{\mathrm{SoC}}}{\sigma t} > \overline{w}_{j,t}^{\mathrm{SoC}}. \tag{31}$$

According to (24), the constraint (27) can be represented by a linear constraint (32) with a one-norm-bounded uncertainty

$$\begin{aligned} P_{j,t}^{\mathrm{chg}} \sigma t - \mathrm{PIO}_{j,t} z_{j,t}^{\mathrm{chg}} \left( \overline{w}_{j,t}^{\mathrm{SoC}} - w_{j,t}^{\mathrm{SoC}} - \alpha \gamma_{j,t} w_{j,t}^{\mathrm{SoC}} \right) \le 0 \\ \forall \gamma_{j,t} : |\gamma_{j,t}|_1 \le 1 \end{aligned} \tag{32}$$

where $P_{j,t}^{\mathrm{chg}}, z_{j,t}^{\mathrm{chg}} \in \boldsymbol{x}$, $\gamma_{j,t} \in \boldsymbol{w}$, $j = 1, \ldots, m$, and $t = 1, \ldots, T$.

The uncertainty parameters in the constraint (32) can be removed by using the fact that $\max_{|\gamma_{j,t}| \le p} w_{j,t}^{\mathrm{SoC}} \gamma_{j,t}$ is $\| w_{j,t}^{\mathrm{SoC}} \|_{p*}$, where $\| \cdot \|_{p*}$ denotes the dual $p$-norm, and $1/p + 1/p^* = 1$ [23]. In this case, $p$ is 1. Therefore, $\| \cdot \|_{p*}$ is the $\infty$-norm. Thus, the constraint (27) is replaced with

$$P_{j,t}^{\mathrm{chg}} \sigma t - \mathrm{PIO}_{j,t} z_{j,t}^{\mathrm{chg}} \left( \overline{w}_{j,t}^{\mathrm{SoC}} - w_{j,t}^{\mathrm{SoC}} - \alpha \left\| w_{j,t}^{\mathrm{SoC}} \right\|_{p*} \right) \le 0 \tag{33}$$

where $P_{j,t}^{\mathrm{chg}}, z_{j,t}^{\mathrm{chg}} \in \boldsymbol{x}$, $j = 1, \ldots, m$, and $t = 1, \ldots, T$. Constraint (33) is linear without uncertainty parameters. Hence, the constraint (27) with uncertainty parameters is replaced with the computable constraints (33) without uncertainty parameters.

Similarly, the constraint (28)–(31) can be replaced with four linear constraints (34)–(37), respectively, without any uncertainty as well

$$P_{j,t}^{\mathrm{dis}} \sigma t - \mathrm{PIO}_{j,t} z_{j,t}^{\mathrm{dis}} \left( w_{j,t}^{\mathrm{SoC}} - \alpha \left\| w_{j,t}^{\mathrm{SoC}} \right\|_{p*} \right) \le 0 \tag{34}$$

$$\begin{aligned} &0 \le R_{j,t}^{d} \le \mathrm{PIO}_{j,t} \\ &\quad \min \left( \overline{P}_{j,t}^{\mathrm{dis}} - P_{j,t}^{\mathrm{dis}} \left( w_{j,t}^{\mathrm{SoC}} - \alpha \left\| w_{j,t}^{\mathrm{SoC}} \right\|_{p*} \right) \Big/ \sigma t - P_{j,t}^{\mathrm{dis}} \right) \end{aligned} \tag{35}$$

$$\begin{aligned} &z_{j,t}^{d\mathrm{Res}} = 0 \text{ if} \\ &\quad \min \left( \overline{P}_{j,t}^{\mathrm{dis}} - P_{j,t}^{\mathrm{dis}} \left( w_{j,t}^{\mathrm{SoC}} - \alpha \left\| w_{j,t}^{\mathrm{SoC}} \right\|_{p*} \right) \Big/ \sigma t - P_{j,t}^{\mathrm{dis}} \right) < R^{\min} \end{aligned} \tag{36}$$

$$z_{j,t}^{c\mathrm{Res}} = 0 \text{ if } P_{j,t}^{\mathrm{chg}} + \frac{w_{j,\mathrm{t}}^{\mathrm{SoC}} - \alpha \left\| w_{j,\mathrm{t}}^{\mathrm{SoC}} \right\|_{p*}}{\sigma t} > \overline{w}_{j,t}^{\mathrm{SoC}}. \tag{37}$$

This completes the process of removing the uncertainties of the RO model (26) and deriving its robust counterpart. The RO problem (26) is therefore reformulated in the following form:

$$\begin{aligned} &\min_{\boldsymbol{x}} \ \hat{f}(\boldsymbol{x}) \\ &\text{s.t } \hat{g}(\boldsymbol{x}) \preccurlyeq 0. \end{aligned} \tag{38}$$

The objective $\hat{f}$ and constraints $\hat{g}$ of the new computable model (38) do not contain any uncertainty. Furthermore, this model is a mixed-integer quadratic programming problem, which can be solved by CPLEX or Gurobi efficiently.

## IV. Numerical Simulations

### A. Simulation System Setup

A ten-generator power grid in [19] is used for simulation studies. The fuel costs and parameters of the thermal generators can be found in [19]. The total installed generation capacity of the system is 1662 MW. The duration of each dispatch interval $t$ is 1 h and the value of $T$ is 24. The 24-h base load curve without PEVs is obtained by scaling the actual hourly loads of the Pennsylvania-New Jersey-Maryland (PJM) interconnection market on July 19th, 2013 [24] with the peak load of 1500 MW in the 12th hour and the valley load of 1107 MW in the 24th hour. Seven generators (units 2–8) provide the reserve service. The reserve requirement is set as $= 3 \times (\max_{t \in T}(P_t^{\mathrm{load}} + \sum_{j=1}^{m} (P_{j,t}^{\mathrm{chg}} - P_{j,t}^{\mathrm{dis}}))\ )^{1/2}$ [25]. $R^{\min}$ is set as 1 MW. Meanwhile, the power grid should provide 30 763 MWh during the day without the PEV loads. The proposed RO model is validated and compared with the DO model through a two-stage process as follows.

*Stage 1:* Obtain the DA generation and reserve schedules for the generators and PEV aggregators using the DO and RO models, respectively. In this stage, the ARIMA model is used

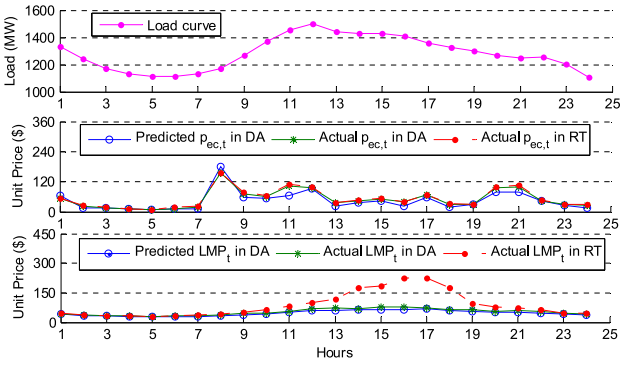


Fig. 1. Curves of base load as well as the capability unit price of reserve and LMP in the DA and RT markets.

to predict the DA hourly regulation market capability prices and LMPs for all PEV aggregators based on the historical data.

*Stage 2:* The DA schedules obtained from the DO and RO models in stage 1 are dispatched on the next day of operation. The generators and PEV aggregators participate in the real-time (RT) balancing market to sell/buy the deviated energy/reserve caused by the uncertain available energy capacities of the PEV aggregators in stage 1. The extra cost incurred in the RT market is calculated by using actual hourly regulation market capability prices and weighted-average LMPs on the day of operation obtained from the PJM market. The extra cost is then added to the total cost of the system described by (1) for the validation and comparison of the DO and RO models.

Fig. 1 shows the curves of the base load, the predicted, and actual capability unit prices of the reserve and LMPs in the DA markets, and the actual capability unit price of the reserve and LMP in the RT market. It can be seen that the predicted DA prices match the actual DA prices with good precision. Furthermore, the RT prices are higher than the corresponding DA prices during most time of the day.

The PEVs in the system are grouped into three aggregators according to their locations based on a survey on the state of New York [26], where aggregators 1–3 cover the areas with the populations less than 5 00 000, between 5 00 000 and 3 million, and more than 3 million, respectively. Furthermore, it is assumed that within the three PEV aggregators, the charging/discharging service can be provided to maximally 1400, 52 000, and 85 000 PEVs, respectively, due to the capacities of the charging/discharging facilities. The parameters of the three PEV aggregators are listed in Table I. The three PEV aggregators participate in the grid operation during 1:00–3:00, 7:00–15:00, and 19:00–24:00, and their PIO values are set to be one in these hours.

### B. Construct Uncertainty Set

Since the historical data of $w_{j,t}^{\mathrm{SoC}}$ are not available, it is unsuitable to use the ARIMA model or other time series prediction methods to predict it. In this paper, the values of $w_{j,t}^{\mathrm{SoC}}$ are obtained by using a Monte Carlo simulation approach [27] based on the stochastic mobility behaviors of the PEVs in the aggregator provided by the survey [26], which include the

TABLE I
PARAMETERS OF THE THREE PEV AGGREGATORS

| Parameter | PEV Aggregators $j$ | | |
|---|---|---|---|
| | 1 | 2 | 3 |
| $\overline{E}_j^{SOC}$ (MWh) | 42 | 1560 | 2550 |
| $\eta_j^{chg}$ | 0.9 | 0.87 | 0.92 |
| $\eta_j^{dis}$ | 0.9259 | 0.9524 | 0.9174 |
| $\overline{P}_j^{chg}$ / $\overline{P}_j^{dis}$ (MW) | 4.2/3 | 156/117 | 255/190 |

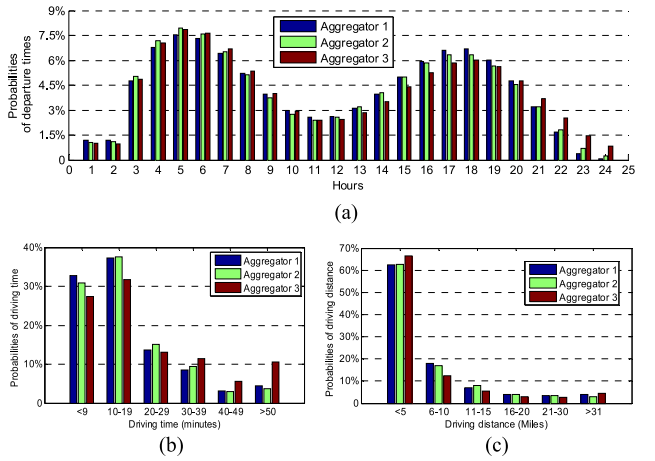


Fig. 2. Stochastic mobility behaviors of the three PEV aggregators: distributions of (a) departure time of daily commutation, (b) daily driving time, and (c) daily driving distance.

probabilities of departure time [Fig. 2(a)] for commutation, driving time [Fig. 2(b)], and driving distance [Fig. 2(c)]. Then, the numbers of PEVs parked in an aggregator during each $t$ can be determined using their departure and driving times. Specifically, in each $t$, the Monte Carlo method is used to statistically generate a certain number (e.g., 500 in this paper) of samples. The value of $w_{j,t}^{\mathrm{SoC}}$ is then calculated to be the average value of the samples. Then, the uncertainty set $\mathcal{R}_j^{\mathrm{SoC}}$ is constructed using (24). The upper and lower bounds of $\tilde{w}_{j,t}^{\mathrm{SoC}}$ of each aggregator are set as 90% and 30% of its maximum energy capacity during each $t$, respectively, by considering the allowable range of the state of charges of the PEVs' batteries during normal operation.

As shown in Fig. 2, the mobility behaviors of the three PEV aggregators are similar. Their departure time distributions all peak around 5:00 and 17:00. Most PEVs are parked from 22:00 to 2:00 of the next day, and around 12:00. These distribution curves coincide with the daily load curve, namely, most PEVs are parked during the peak-load and valley-load periods within a day. Therefore, it is preferable to charge PEVs during the valley-load period (from 23:00 to 2:00 of the next day), and discharge PEVs during the peak-load period (around 12:00) if necessary. Furthermore, a PEV aggregator can participate in the grid operation to supply load when it is in the discharging mode, or provide regulation reserve when it is in the charging or discharging mode.

According to (24) and (27)–(31) and the parameters of each PEV aggregator in Table I, the uncertainty set (the predicted value and upper and lower bounds) of the available

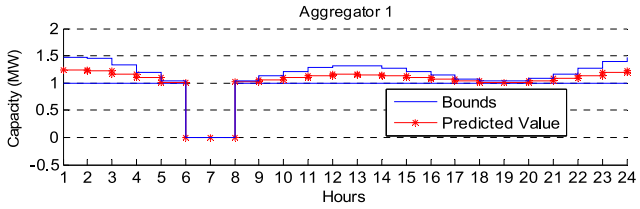


Fig. 3. Uncertainty set of the available reserve capacity of aggregator 1.

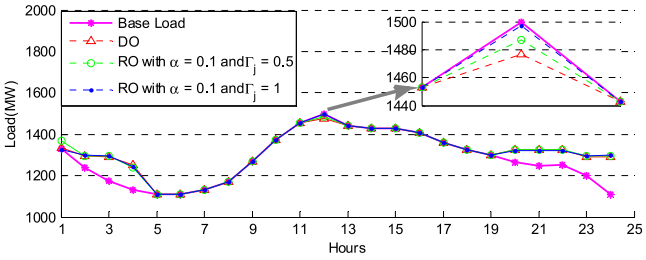


Fig. 4. Comparison of load profiles for four cases during 24 h.

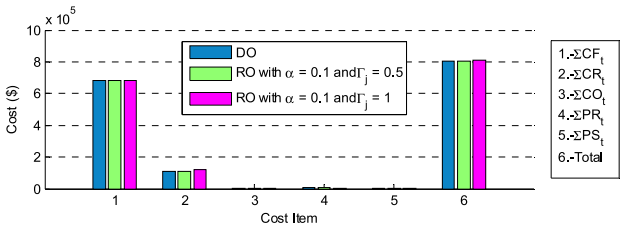


Fig. 5. Comparison of the itemized costs and the objective function values of the DO and RO cases.

reserve capacity of each aggregator can be obtained from $\mathcal{R}_j^{\text{SoC}}$. As an example, Fig. 3 shows the uncertainty set of the available reserve capacity of the PEV aggregator 1, where the stochastic mobility behavior of every PEV in this aggregator is assumed to follow the standard uniform distribution, $R^{\min}$ is set to be 1 MW, and $\alpha = 0.1$. The curve with stars corresponds to $\Gamma_j = 0$; and the area between the two bounds covers all possible values of the available reserve capacity when $\Gamma_j = 1$. In general, a larger $\alpha$ leads to a wider area between the two bounds. However, when the low bound of the area is lower than $R^{\min}$, the available reserve capacity will be empty, such as during 6:00–8:00 in Fig. 3, which means aggregator 1 will not participate in the regulation reserve service during these hours.

### C. Case Study

The proposed RO model is programmed in MATLAB 2012a and solved using Gurobi 5.1 on a 3.4 GHz desktop computer with a 16-G RAM. The relative gap between the lower and upper objective bounds of Gurobi is set to be 1%. In this paper, the average combined fuel economy of PEVs is 30 kWh/100 miles [2]. Therefore, the daily energy consumption $E_j^{\text{Con}}$ of each PEV aggregator $j$ can be estimated according to the driving time [Fig. 2(b)] and driving distance [Fig. 2(c)], and the results are 8.4, 213, and 510 MWh for the PEV aggregators 1–3, respectively. Each of them is roughly 20% of the maximum available energy capacity of the PEV aggregator.

*1) Model Validation in Stage 1:* Fig. 4 compares the load profiles for four cases in stage 1 of validation: the base load case (no PEVs), the case when the DO model is used, and the cases when the RO model with $\alpha = 0.1$ and $\Gamma_j = 0.5$ or $\Gamma_j = 1$ are used, where $j = 1,\ 2,\ 3$. In the DO and RO cases, the discharging power from the PEV aggregators is considered as a negative load. The differences between the base load curve and three other curves indicate that the PEV aggregators are charged during the valley hours, which are 1:00–3:00 and 19:00–24:00, in the DO or RO cases. In some valley hours, e.g., 5:00–7:00, the PIO statuses of the PEV aggregators are set to be zero because most PEVs depart during those hours according to Fig. 2(a) and, therefore, cannot be charged or participate in the grid operation. Furthermore, since the PEV aggregators in the DO and RO cases provide discharging power to the grid during 11:00–12:00, the peak load is reduced. Compared to the RO cases, the PEV aggregators provide more discharging power in the DO case, which is anticipated in stage 1 DA scheduling because the predicted available energy capacity of V2G is assumed to be accurate in the DO model but has uncertainty in the RO model. Moreover, in the RO cases, the discharging power reduces with the increase of the uncertainty level. These results clearly show the benefits of the V2G as a consequence of using the bidirectional dispatch coordination: the extra cost of using expensive generation to meet the peak load demand is reduced; and the ramp-up/down costs of thermal generators are also reduced because the load curves are flattened by V2G.

*2) Comparison of the DO and RO Models:* Fig. 5 compares the itemized and total costs of the DO case and the two RO cases in stage 1, where the predicted available energy capacities of the PEV aggregators used in the DO case are assumed accurate. Owing to the fast response and no extra costs for ramp-up/down, the PEV aggregators (other than extra high-cost generators) are selected to fulfill the spinning reserve requirement. As Fig. 5 shows, the objective function values of the RO cases are slightly higher than that of the DO case.

However, the operation schedules obtained from the DO model are risky when the available reserve capacities of some PEV aggregators suffer negative forecast errors such that they cannot provide the scheduled spinning reserve capacities or discharging power during some hours in the next day of actual dispatch. In this case, the PEV aggregators will participate in the RT balancing market to compensate their energy/reserve deviations, as described in stage 2. This may lead to an increase of the actual total system cost (i.e., the objective function value) in the next day of operation.

Compared to the DO model, since the uncertainties have been considered in the RO model, less adjustment to the DA schedules is needed in the RT market. Therefore, the objective function values of the RO cases in the next day of operation are less than that of the DO case. Fig. 6 shows the percentage increase of the objective function value of the DO model in the next day of operation (stage 2) against that

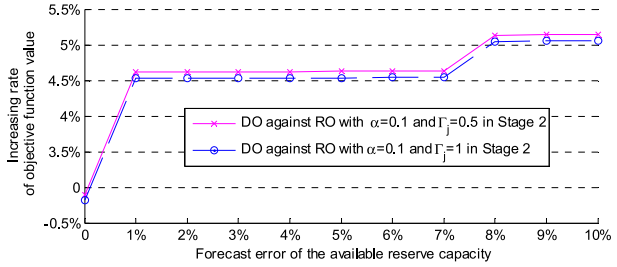


Fig. 6. Percentage increase of the objective function value of the DO model against that of the RO model versus the forecast error of the total available reserve capacity of the PEV aggregators in the day of operation.

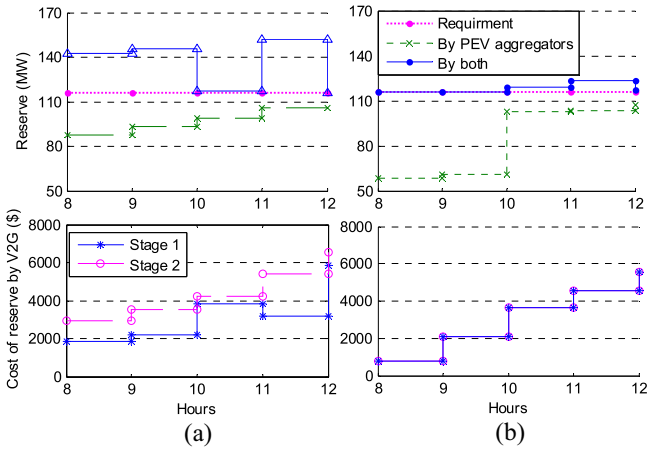


Fig. 7. Adjusted reserve schedules in stage 2 as well as the costs of reserve in different stages obtained from (a) DO model and (b) RO model with $\alpha = 0.1$ and $\Gamma_j = 0.5$ during 8:00–12:00 when there is $-5\%$ forecast error in the total available reserve capacity of the PEV aggregators.

of the RO model versus the negative forecast error of the total available reserve capacity of the PEV aggregators from 0 to 10% (with an increment of 1%), where the RO model ($\alpha = 0.1$) with $\Gamma_j = 0.5$ and $\Gamma_j = 1$ ($j = 1,\ 2,\ 3$) has considered the forecast error in the range of $\pm 5\%$ and $\pm 10\%$, respectively. The objective function value of the DO model is slightly lower than that of the RO model if there is no forecast error, but is 4.5% more than that of the RO model even in the case of $-1\%$ forecast error. Since a forecast error is inevitable, the RO model is robust and more economic than the DO model for scheduling the operations of the generators and PEV aggregators.

As an example, Fig. 7 compares the adjusted reserve schedules in stage 2 as well as the costs of reserve provided by the PEV aggregators in stages 1 and 2 obtained from the DO model and the RO model with $\alpha = 0.1$ and $\Gamma_j = 0.5$ during 8:00–12:00 when there is $-5\%$ forecast error in the total available reserve capacity of the PEV aggregators. When the DO model is used, since the uncommitted generators have high start-up cost and/or slow response, the PEV aggregators commit to provide the reserve capacity. As a result, the total reserve capacity provided by both generators and PEV aggregators in the next day of operation is higher than the actual reserve requirement due to the negative forecast error of the total available reserve capacity of the PEV aggregators, leading to an increase of the spinning reserve cost,

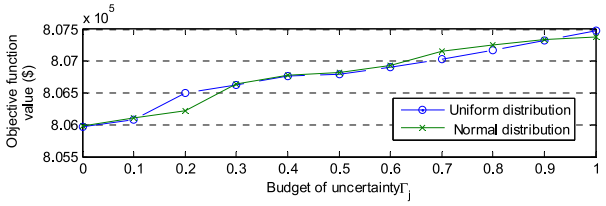


Fig. 8. Comparison of the objective function values for different budgets of uncertainty when the PEV mobility behaviors are modeled by uniform and normal distributions.

as shown in Fig. 7(a). In contrast, since the RO model has covered the $-5\%$ forecast error, no reserve adjustment is needed in stage 2, and the resulting scheduled reserve capacity in the next day of operation is close to the requirement, which avoids the increase of the spinning reserve cost, as shown in Fig. 7(b).

*3) Robustness to the Probability Model of the PEV Mobility:* The probability distribution model of the stochastic mobility behaviors of the PEVs in a PEV aggregator can affect the prediction accuracy of the PEV aggregator's available energy capacity. It is desired that the RO model is robust to the probability distribution model of the PEV mobility. To evaluate such robustness of the RO model, the Monte Carlo simulation approach described in Section IV-B is used to obtain two different uncertainty sets of the hourly available energy capacity for each PEV aggregator on July 19, 2013 by assuming that the mobility of the PEVs follows the commonly used standard uniform and normal distributions, respectively. For the normal distribution, the mean of the hourly available energy capacity of each aggregator is set to be 70% of the maximum energy capacity of the PEV aggregator during the hour, and the standard deviation is set as 4% of the mean. The process of generating the uncertain sets of $\tilde{w}_{j,t}^{\mathrm{SoC}}$ has been discussed in Section IV-B, where the value of $\alpha$ is chosen to be 0.1.

Fig. 8 compares the objective function values of using two different distributions to model the stochastic PEV mobility when $\alpha = 0.1$ and $\Gamma_j$ increases from 0 to 1 with an increment of 0.1. The maximum difference of the objective function values of the two cases is only 0.36%.

When using a certain probability distribution to model the PEV mobility, the parameters of the distribution may also affect the prediction accuracy of the PEV aggregator's available energy capacity. In this paper, the mean of the normal distribution is set to be 70% of the maximum energy capacity of each PEV aggregator in each hour, but 11 different standard deviations from 0% to 40% of the mean value with an increment of 4% are chosen for the Monte Carlo simulation. Using the aforementioned process, 11 different uncertainty sets of the hourly available energy capacity are obtained for each PEV aggregator. Then, the RO model with $\alpha = 0.1$ and $\Gamma_j$ changing from 0 to 1 with an increment of 0.1 is simulated to obtain the operation schedules of the generators and PEV aggregators using each uncertainty set. The objective function value of the next day of operation obtained in stage 2 versus the standard deviation of the PEV mobility distribution and the budget of uncertainty is shown in Fig. 9. The maximum difference of the

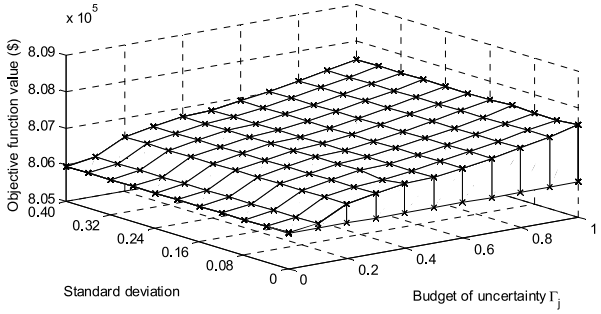


Fig. 9. Objective function value of the RO model versus standard deviation of the normal PEV mobility distribution and budget of uncertainty.

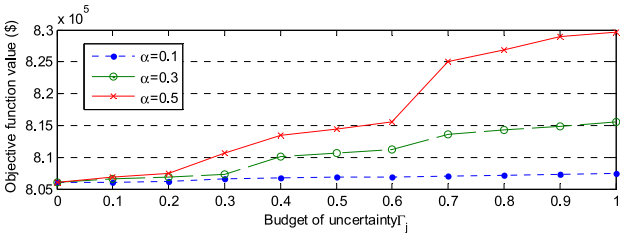


Fig. 10. Comparison of objective function values of the RO model versus budget of uncertainty at different levels of uncertainty.

objective function values for different uncertainty sets under the same budge of uncertainty is only 0.01%.

The results in Figs. 8 and 9 indicate that the uncertainties of the PEV aggregators' available energy capacities caused by the uncertain PEV mobility have been well covered by the proposed RO model, regardless what probability distribution models and parameters are used to model these uncertainties. Thus, the proposed RO model (20) is robust to the probability distribution modeling of the PEV mobility.

*4) Effects of the Parameters of Uncertainty:* Fig. 10 illustrates the curves of the objective function value obtained from the RO model versus $\Gamma_j$ changing from 0 to 1 with an increment of 0.1 when the value of $\alpha$ is 0.1, 0.3, and 0.5. When $\alpha = 0.1$ or 0.3, the objective function value increases slowly as $\Gamma_j$ increases. Even when $\Gamma_j = 1$, which indicates a large prediction error, the objective function value increases no more than 0.19% and 1.22%, respectively, with respect to that when $\Gamma_j = 0$. However, this increase reaches 3.1% when $\alpha = 0.5$. The results show that by coordinating the charging and discharging operations of the PEV aggregators, the uncertain behaviors of the PEVs have a low impact on the operation cost of the power grid when the uncertainty level of the PEV mobility is moderate, e.g., less than 0.3. Such an impact can be further mitigated by improving the prediction accuracy in practice. The results also reveal that for the same uncertainty level (i.e., $\alpha \times \Gamma_j$ is constant), it is better to use a lower $\alpha$ and higher $\Gamma_j$ than using a higher $\alpha$ and lower $\Gamma_j$.

*5) Impact of the Uncertain Price Volatility:* Since the proposed RO model only considers the uncertainty of $w_{j,t}^{\mathrm{SoC}}$, it is worth to investigate the impact of other uncertainties, such as the uncertain volatilities of the reserve capability unit prices ($p_{ec,t}$) and LMPs ($\mathrm{LMP}_{j,t}$), on the dispatch result. Two tests are performed to investigate the impact. In the first test,

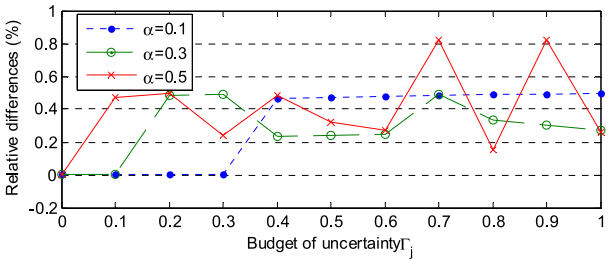


Fig. 11. Relative differences of the objective function values of the cases in the second test with respect to that of the base case versus budget of uncertainty $\Gamma_j$ for three different values of $\alpha$.

the proposed RO model with the actual $p_{ec,t}$ and $\mathrm{LMP}_{j,t}$ is solved and the resulting optimal solution and objective function value reflect the case when there is no uncertain volatility in the prices, which is called the base case. In the second test, the proposed RO model with the predicted $p_{ec,t}$ and $\mathrm{LMP}_{j,t}$ is solved for different uncertain levels (i.e., different combinations of $\alpha$ and $\Gamma_j$ values) of $w_{j,t}^{\mathrm{SoC}}$. Then, the objective function values of the RO model are recalculated using the actual $p_{ec,t}$ and $\mathrm{LMP}_{j,t}$ for different cases to represent the dispatch results when the uncertain volatilities of the prices are considered. The relative differences in percentage of the objective function values of the cases in the second test with respect to that of the base case are plotted as functions of $\Gamma_j$ for three different $\alpha$ values in Fig. 11, where $\Gamma_j$ changes from 0 to 1 with an increment of 0.1. The results indicate that the relative differences of the objective function values are less than 0.5% in most cases with price uncertainties. The maximum relative difference between the two tests is only 0.82%. Thus, the impact of the uncertain price volatilities is much less than that of the uncertain PEV mobility as shown in Fig. 6 when the DO model is used. Nevertheless, as discussed in Section II-C, the uncertainties of the prices can be considered in the same way as the uncertainty of $w_{j,t}^{\mathrm{SoC}}$ in the proposed RO model if necessary.

*6) Benefit of the RO Model to the PEV Owners:* The results in Sections IV-C2-Section IV-C5 have demonstrated the benefit of the RO model in minimizing the total cost of the system from the perspective of the grid operator. However, the satisfaction of the PEV owners in an aggregator is also important to evaluate the benefit of the RO model. The PEV owners will be satisfied if they meet their charging requirement while gaining as much revenues as possible from participating in the power grid operation. The revenues of the PEVs are considered as a kind of operation cost in the proposed DO and RO models, which are $\mathrm{PR}_t$ and $\mathrm{PS}_t$ in the objective function (1). However, if a PEV aggregator cannot provide all of the reserve capacity scheduled in the DA market (stage 1), it will have to buy the deviated reserve capacity in the RT market (stage 2) from other providers, such as expensive generators. This will cause an extra cost or a loss of the revenue for the PEV aggregator. The extra cost can be reflected by the variation of $\mathrm{CR}_t + \mathrm{CO}_t$ between stages 1 and 2.

Fig. 12 compares $\mathrm{PR}_t + \mathrm{PS}_t$ and $\mathrm{CR}_t + \mathrm{CO}_t$ separately in different stages obtained from the DO and RO models, where $\alpha = 0.1$ and $\Gamma_j = 0.5$ are used in the RO model and there

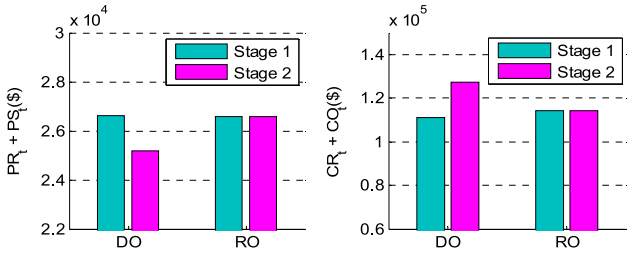


Fig. 12. Comparison of the revenue of the PEV aggregators and the cost of the generators in the two stages using the DO and RO models.

is a $-5\%$ forecast error in the total available reserve capacity of the PEV aggregators. The results show that the value of $\mathrm{PR}_t + \mathrm{PS}_t$ in stage 2 decreases 5.3% compared with that in stage 1 when using the DO model, but remains the same when using the RO model. Meanwhile, the total cost of the thermal generators to provide the reserve capacity ($\mathrm{CR}_t$) and the startup and shutdown cost ($\mathrm{CO}_t$) using the DO model increases 12.6% in stage 2, leading to revenue losses of the PEV aggregators. On the contrary, the total cost of $\mathrm{CR}_t + \mathrm{CO}_t$ remains the same in stages 1 and 2 when using the RO model. As a result, the total objective function value in stage 2 increased 4.6% compared with that in stage 1 when using the DO model, which coincides with the results in Fig. 6. These results demonstrate that the PEV aggregators are more satisfied by using the RO model than using the DO model because the RO model enables the PEV owners to gain more revenues in the RT market.

## V. Conclusion

This paper has proposed an RO model for bidirectional dispatch coordination of PEVs in a power grid. The RO model has taken into account the uncertainty of the stochastic mobility of the PEVs and the logical relations among charging, discharging, and providing regulation reserve of each PEV aggregator. The proposed RO model has been reformulated as a deterministic mixed-integer quadratic programming problem, which can be solved efficiently by using a state-of-the-art solver, such as CPLEX or Gurobi. Numerical experiments have been conducted for a power grid with ten thermal generators and three PEV aggregators to evaluate the proposed RO model. Results have shown that optimally coordinating PEV charging/discharging with thermal generators and the ability of PEV aggregators to provide regulation reserve service are beneficial to power grid operation in terms of eliminating the influence of uncertainty on the overall cost while satisfying the transportation requirement of the PEVs. Moreover, the proposed RO model is robust to the probability modeling of the uncertain PEV mobility.

## References

[1] W. Kempton and S. E. Letendre, "Electric vehicles as a new power source for electric utilities," *Transp. Res. D Transp. Environ.*, vol. 2, no. 3, pp. 157–175, Sep. 1997.

[2] W. Kempton and J. Tomić, "Vehicle-to-grid power fundamentals: Calculating capacity and net revenue," *J. Power Sources*, vol. 144, no. 1, pp. 268–279, Jun. 2005.

[3] W. Kempton and J. Tomić, "Vehicle-to-grid power implementation: From stabilizing the grid to supporting large-scale renewable energy," *J. Power Sources*, vol. 144, no. 1, pp. 280–294, Jun. 2005.

[4] C. D. White and K. M. Zhang, "Using vehicle-to-grid technology for frequency regulation and peak-load reduction," *J. Power Sources*, vol. 196, no. 8, pp. 3972–3980, Apr. 2011.

[5] Y. Ma, T. Houghton, and A. Cruden, "Modeling the benefits of vehicle-to-grid technology to a power system," *IEEE Trans. Power Syst.*, vol. 27, no. 2, pp. 1012–1020, May 2012.

[6] E. Sortomme and M. A. El-Sharkawi, "Optimal combined bidding of vehicle-to-grid ancillary services," *IEEE Trans. Smart Grid*, vol. 3, no. 1, pp. 70–79, Mar. 2012.

[7] S. Han, "Development of an optimal vehicle-to-grid aggregator for frequency regulation," *IEEE Trans. Smart Grid*, vol. 1, no. 1, pp. 65–72, Jun. 2010.

[8] T. K. Kristoffersen, K. Capion, and P. Meibom, "Optimal charging of electric drive vehicles in a market environment," *Appl. Energy*, vol. 88, no. 5, pp. 1940–1948, May 2011.

[9] A. Y. Saber, "Plug-in vehicles and renewable energy sources for cost and emission reductions," *IEEE Trans. Ind. Electron.*, vol. 58, no. 4, pp. 1229–1238, Apr. 2011.

[10] M. W. Khalid, A. T. Al-Awami, and E. Sortomme, "Stochastic-programming-based bidding strategy for V2G services," in *Proc. 4th IEEE/PES Innov. Smart Grid Technol. Eur.*, Lyngby, Denmark, Oct. 2013, pp. 1–5.

[11] M. E. Khodayar, L. Wu, and M. Shahidehpour, "Hourly coordination of electric vehicle operation and volatile wind power generation in SCUC," *IEEE Trans. Smart Grid*, vol. 3, no. 3, pp. 1271–1279, Sep. 2012.

[12] A. Ben-Tal, L. E. Ghaoui, and A. Nemirovski, *Robust Optimization*. Princeton, NJ, USA: Princeton Univ. Press, 2009.

[13] S. Dehghan, N. Amjady, and A. Kazemi, "Two-stage robust generation expansion planning: A mixed integer linear programming model," *IEEE Trans. Power Syst.*, vol. 29, no. 2, pp. 584–597, Mar. 2014.

[14] D. Bertsimas, E. Litvinov, X. A. Sun, J. Zhao, and T Zheng, "Adaptive robust optimization for the security constrained unit commitment problem," *IEEE Trans. Power Syst.*, vol. 28, no. 1, pp. 52–63, Feb. 2013.

[15] C. Lee, C. Liu, S. Mehrotra, and M. Shahidehpour, "Modeling transmission line constraints in two-stage robust unit commitment problem," *IEEE Trans. Power Syst.*, vol. 29, no. 3, pp. 1221–1231, May 2014.

[16] Y. Guan and J. Wang, "Uncertainty sets for robust unit commitment," *IEEE Trans. Power Syst.*, vol. 29, no. 3, pp. 1439–1440, May 2014.

[17] (Mar. 2014). *IBM ILOG CPLEX 12.4*. [Online]. Available: http://www-01.ibm.com/

[18] (Mar. 2014). *Gurobi Optimizer 5.1*. [Online]. Available: http://www.gurobi.com

[19] C.-P. Cheng, C.-W. Liu, and C.-C. Liu, "Unit commitment by Lagrangian relaxation and genetic algorithms," *IEEE Trans. Power Syst.*, vol. 15, no. 2, pp. 707–714, May 2000.

[20] (Jun. 2005). *Minimum Up/Down Polytopes of the Unit Commitment Problem With Start-Up Costs, IBM Research Report.* [Online]. Available: http://domino.research.ibm.com/library/cyberdig.nsf/papers/CDCB02A7C809D89E8525702300502AC0/$File/rc23628.pdf

[21] A. J. Conejo, M. Carrión, and J. M. Morales, *Decision Making Under Uncertainty in Electricity Markets*. New York, NY, USA: Springer, 2010.

[22] A. Ben-Tal and A. Nemirovski, "Robust optimization-methodology and applications," *Math. Prog.* vol. 92, no. 3, pp. 453–480, May 2002.

[23] S. Boyd and L. Vandenberghe, *Convex Optimization*. Cambridge, U.K.: Cambridge Univ. Press, 2004.

[24] (Dec. 2013). *PJM Energy Market Data*. [Online]. Available: http://www.pjm.com/ markets-and-operations/energy.aspx

[25] Y. Rebours and D. Kirschen, "A survey of definitions and specifications of reserve services," Report, Univ. of Manchester, Oct. 2005.

[26] (Jun. 2012). *New York State 2009 NHTS Comparison Report*. [Online]. Available: https://www.dot.ny.gov/divisions/policy-and-strategy/darb/dai-unit/ttss/repository/ComparisonRpt09-95-011107.pdf

[27] D. Dallinger, D. Krampe, and M. Wietschel, "Vehicle-to-grid regulation reserves based on a dynamic simulation of mobility behavior," *IEEE Trans. Smart Grid*, vol. 2, no. 2, pp. 302–313, Jun. 2011.

**Xiaoqing Bai** received the B.S. degree in software engineering and the Ph.D. degree in electrical engineering, in 1991 and 2010, respectively, both from Guangxi University, Nanning, China.

She is currently a Post-Doctoral Research Associate with the Department of Electrical and Computer Engineering, University of Nebraska–Lincoln, Lincoln, NE, USA. She was with Guangxi Key Laboratory of Power System Optimization and Energy Technology, Guangxi University. Her current research interests include optimization theories and their applications in power systems.

**Wei Qiao** (S'05–M'08–SM'12) received the B.E. and M.E. degrees in electrical engineering from Zhejiang University, Hangzhou, China, in 1997 and 2002, respectively; the M.S. degree in high performance computation for engineered systems from Singapore-MIT Alliance, Singapore; and the Ph.D. degree in electrical engineering from the Georgia Institute of Technology, Atlanta, GA, USA, in 2003 and 2008, respectively.

Since 2008, he has been with the University of Nebraska–Lincoln (UNL), Lincoln, NE, USA, where he is currently an Associate Professor in the Department of Electrical and Computer Engineering. His current research interests include renewable energy systems, smart grids, microgrids, condition monitoring, energy storage systems, power electronics, electric machines and drives, and computational intelligence. He has authored/co-authored three book chapters and over 140 papers in refereed journals and international conference proceedings, and has five international/U.S. patents pending.

Dr. Qiao was the recipient of the 2010 U.S. National Science Foundation CAREER Award, the 2010 IEEE Industry Applications Society (IAS) Andrew W. Smith Outstanding Young Member Award, the 2012 UNL College of Engineering Faculty Research and Creative Activity Award, the 2011 UNL Harold and Esther Edgerton Junior Faculty Award, and the 2011 UNL College of Engineering Edgerton Innovation Award. He was also the recipient of four best paper awards from IEEE IAS, Power and Energy Society, and Power Electronics Society. He is an Associate Editor of the IEEE TRANSACTIONS ON ENERGY CONVERSION, *IET Power Electronics*, and the IEEE JOURNAL OF EMERGING AND SELECTED TOPICS IN POWER ELECTRONICS. He is the Corresponding Guest Editor of a special section on Condition Monitoring, Diagnosis, Prognosis, and Health Monitoring for Wind Energy Conversion Systems of the IEEE TRANSACTIONS ON INDUSTRIAL ELECTRONICS. He was also an Associate Editor of the IEEE TRANSACTIONS ON INDUSTRY APPLICATIONS from 2010 to 2013.